Effects of Notch Root Radius and Stress Ratio on the Fatigue Crack Propagation Threshold for the Short Crack at the Notch Root

Akimitsu Seo[1, a], Masanobu Kubota[2, 3, 4, 5, b] and Yoshiyuki Kondo[2, 3, 5, c]

[1] Graduate School of Kyushu University.

[2] Department of Mechanical Engineering, Kyushu University.

[3] International Institute for Carbon-Neutral Energy Research (I2CNER).

[4] Air Liquide Industrial Chair on Hydrogen Structural Materials and Fracture.

[5] The National Institute of Advanced Industrial Science and Technology (AIST).

744 Motooka, Nishi-ku, Fukuoka, 819-0395, Japan.

[a] 2TE11382E@s.kyushu-u.ac.jp, [b] kubota@mech.kyushu-u.ac.jp,

[c] kondo.yoshiyuki.804@m.kyushu-u.ac.jp

Keywords: Fatigue, Short Crack, Threshold, Notch, Stress Ratio, Crack Closure.

Abstract. The **c**rack growth threshold, ΔK_{th}, for the short crack at the root of a long notch including the effects of notch root radius, ρ, and stress ratio, R, were investigated in this study. The pre-crack, with a depth of 0.15mm, was introduced at the root of a 2mm deep notch which had the root radius changed from 0.015mm to 15mm. A crack propagation test using the unloading elastic compliance method was carried out with the stress ratios of -1, 0 and 0.62 - 0.72 (high R). The material was normalized 0.25 % carbon steel. The change in ΔK_{th} with the change in ρ was dependent on R. Under R = -1, there was a reduction in ΔK_{th} when the notch root radius was greater than 0.5mm. On the other hand, for R = 0 and high R, ΔK_{th} was almost constant regardless of ρ. Although ΔK_{th} was different depending on the stress ratio and notch root radius, the effective crack growth threshold $(\Delta K_{eff})_{th}$ was constant under all the test conditions. Therefore, the change in the crack growth behavior of the short crack at the notch root was dominated by the crack closure. The reduction in ΔK_{th} in the relatively dull notch for R = -1 could also be explained by the change in the development of the crack closure during crack growth.

Introduction

The short crack problem in which a short crack can propagate if the stress intensity factor range was lower than the threshold stress intensity factor range, ΔK_{th} for a long crack is one of the major issues in the design of mechanical components. Many researchers have been challenged to characterize the phenomena and to understand the mechanism of this problem [1]-[5]. However, the crack growth behavior of a short crack has not yet been clarified when the short crack exists in the large stress concentration area such as the long notch root. The objective of this study is to investigate the effect of the notch root radius and stress ratio on the crack propagation threshold, ΔK_{th}, for a short crack at the root of a long notch.

Experimental Procedure

Test material. The material used in this study was 0.25% carbon steel which is designated as S25C by Japanese Industrial Standards. The chemical composition is shown in Table 1. The heat treatment was normalizing at 1143 K. After the introduction of a pre-crack, the specimen received stress relief

annealing at 863 K for 1 h. The mechanical properties and Vickers hardness after the stress relief annealing are shown in Table 2.

Test specimen. The configuration of the specimen, the details of the notch and short pre-crack are shown in Fig. 1. The preparation of the short fatigue pre-crack was as follows: a notch, which was 2mm deep with a 0.015mm notch root radius, was machined through the thickness of the specimen. A 0.15mm deep crack was then introduced by a fatigue test using the unloading elastic compliance method [6] by strain gages which were sticked on the back face of the notch and the nominal part of the specimen. The shape of the notch was then reproduced by machining. The notch root radius used in this experiment was from 0.015mm to 15mm. No additional machining was applied when the notch root radius was 0.015 mm. Finally, stress relief annealing was carried out at 875K for 1 hour in a vacuum to relieve the residual stress at the pre-crack tip and the effect of machining. Fig. 1 (c) shows the pre-crack observed at the fracture surface of the specimen. Preparation of a 0.15mm deep pre-crack, which was through the thickness, was confirmed.

Fatigue crack propagation test. A bending fatigue test machine using an electro-dynamic vibrator was used in the fatigue crack propagation test. The test frequency was 25Hz. The test was done in air at ambient temperature. The fatigue test was terminated as the fatigue limit if no failure of the specimen occurred after 10^7 cycles. The crack length and crack closure behavior were continuously measured by the elastic unloading compliance method [6]. The unloading compliance method using a back face strain gage could not be used for the specimen with a 15mm notch root radius, because of an insufficient sensitivity. The stress ratio was chosen as R = -1, R = 0 and high R (R = 0.62 - 0.72). The high R means that the fatigue test was carried out with a constant mean stress, σ_m, which was 200MPa.

Table 1 Chemical composition of the test material (mass %).

Material	C	Si	Mn	P	S
JIS S25C	0.27	0.17	0.46	0.016	0.018

Table 2 Mechanical properties and Vickers hardness of the test material after stress relief annealing.

Material	Yield strength, $\sigma_{0.2}$ [MPa]	Ultimate tensile strength, σ_B [MPa]	Elongation, δ [%]	Reduction of area, ϕ [%]	Vickers hardness, HV
JIS S25C	300	497	34.5	62.0	140

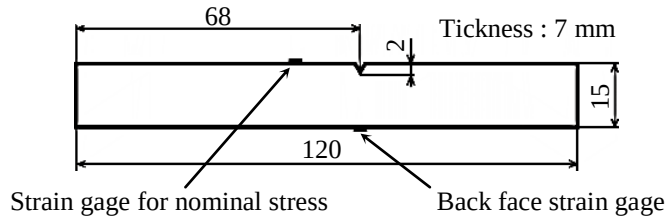

(a) Configuration of specimen

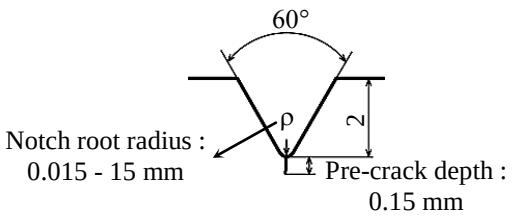

(b) Detail of notch.

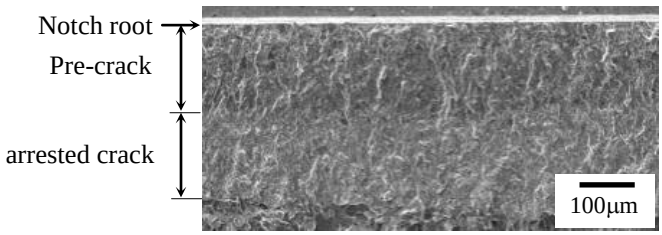

Test conditions for the photo

Pre-crack length 0.15 mm
R = -1
ρ = 0.015 mm
σ_a = 60 MPa (At fatigue limit)
N = 10^7 cycles

(c) Shape and depth of pre-crack

Fig. 1 Notched fatigue test specimen with a short pre-crack (Dimensions are in mm).

Test Results

Effect of notch root radius ρ and stress ratio *R* on threshold stress intensity factor range ΔK_{th}. Fig. 2 shows an example of the *S-N* diagram for this test. The stress amplitude was the nominal value at the notch root. The fatigue limit was changed depending on the stress ratio as well as the notch root radius. The fatigue limits for all the test conditions are shown in Fig. 3. The fatigue limit decreased with the decreasing ρ, and then it leveled off. The fracture surfaces of the fatigue limit specimens were uncovered, and then the crack length was measured on the fracture surface. Thus, ΔK_{th} was calculated by the stress amplitude corresponding to the fatigue limit and the crack length confirmed at the fracture surface. For the calculation of the stress intensity factor, *K*, Gross & Srawley's formula $K=\sigma\times(\pi a)^{1/2}\times\{(1.122\text{-}1.4(a/w)+7.33(a/w)^2\text{-}13.08(a/w)^3+14(a/w)^4\}$ [7] was used for the crack which was shorter than ρ. In the equation, *w* is the width of the specimen and *a* is the crack length. For crack longer than ρ, Lucas & Klesnil's formula $K=1.12\times K_t\times\sigma\times(\pi a)^{1/2}/(1+4.5a/\rho)^{1/2}$ [8] was used. K_t is the stress concentration factor of the notch. Fig. 4 shows ΔK_{th} of all the test conditions. For R = -1, there is a reduction in ΔK_{th} when ρ was greater than 0.5 mm. On the other hand, the ΔK_{th} for R = 0 and high R was almost constant regardless of ρ.

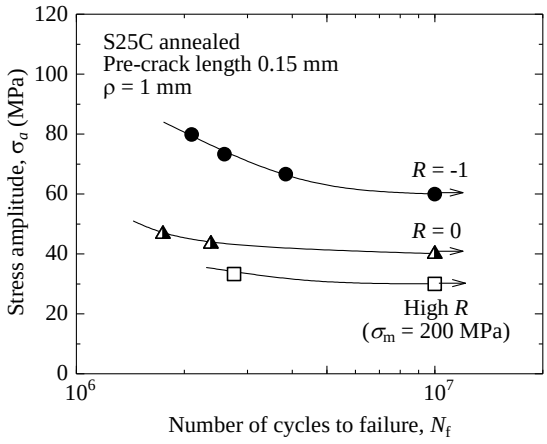

Fig. 2 *S-N* diagram (ρ = 1 mm).

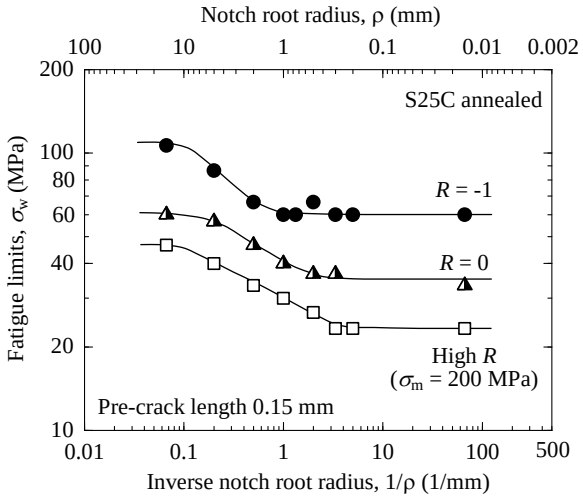

Fig. 3 Fatigue limit σ_w of notched specimen with a short pre-crack.

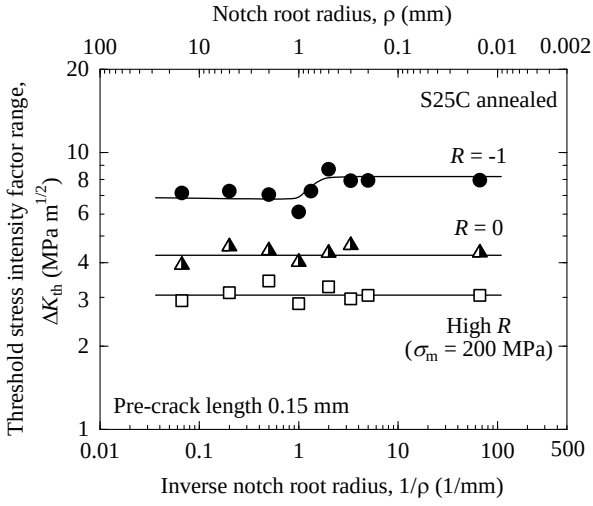

Fig. 4 Effect of notch root radius ρ and stress ratio *R* on ΔK_{th} for a short crack at the notch root.

Evaluation of the effect of notch root radius ρ and stress ratio *R* on fatigue limit threshold by effective threshold stress intensity factor range (ΔK_{eff})$_{th}$. In this experiment, the fatigue limit for R = -1 and R = 0 was achieved by arrest of the fatigue crack growth regardless of the notch root radius. Figure 5 shows the stress-offset displacement curve of the unloading elastic compliance method for the arrested crack at the fatigue limit. The knee point of the curves denotes the crack opening point. That is, the crack tip opens above this point and it closes below this point. In the figure, the short horizontal bars are presented to clearly show the knee point. For R = -1 and R = 0, the development of crack closure was found. For R = -1, the stress range, while crack opens, is relatively lower in the sharp notches than in the dull notches. On the other hand, the stress-offset displacement curves for a high R were straight, thus there was no crack closure.

Figure 6 shows the relationship between the stress ratio, R, and crack opening ratio, U, for the arrested crack at the fatigue limit. The crack opening ratio, in other words, the development of crack closure depended on the stress ratio. In the figure, the open symbols denote the crack opening ratio for the relatively dull notches and the solid symbols are for the relatively sharp notches. For R = -1, the value of U is higher for the dull notches than for the sharp notches. For a high R, the value of U is the same for all notches since there was no crack closure.

The effective threshold stress intensity factor range $(\Delta K_{eff})_{th}$ was calculated by the equation $(\Delta K_{eff})_{th} = U \times \Delta K_{th}$, and the results are shown in Fig. 7. $(\Delta K_{eff})_{th}$ was constant regardless of the notch root radius, ρ, and the stress ratio R. There was a significant difference in ΔK_{th} depending on the stress ratio as shown in Fig. 3. In the figure, the reduction of ΔK_{th} was also found for R = -1. However, $(\Delta K_{eff})_{th}$ for R = -1 and R = 0 are equivalent to that for the high R in which crack closure did not occur. Therefore, the behavior of ΔK_{th} for a short crack at the notch root was dominated by the crack closure behavior.

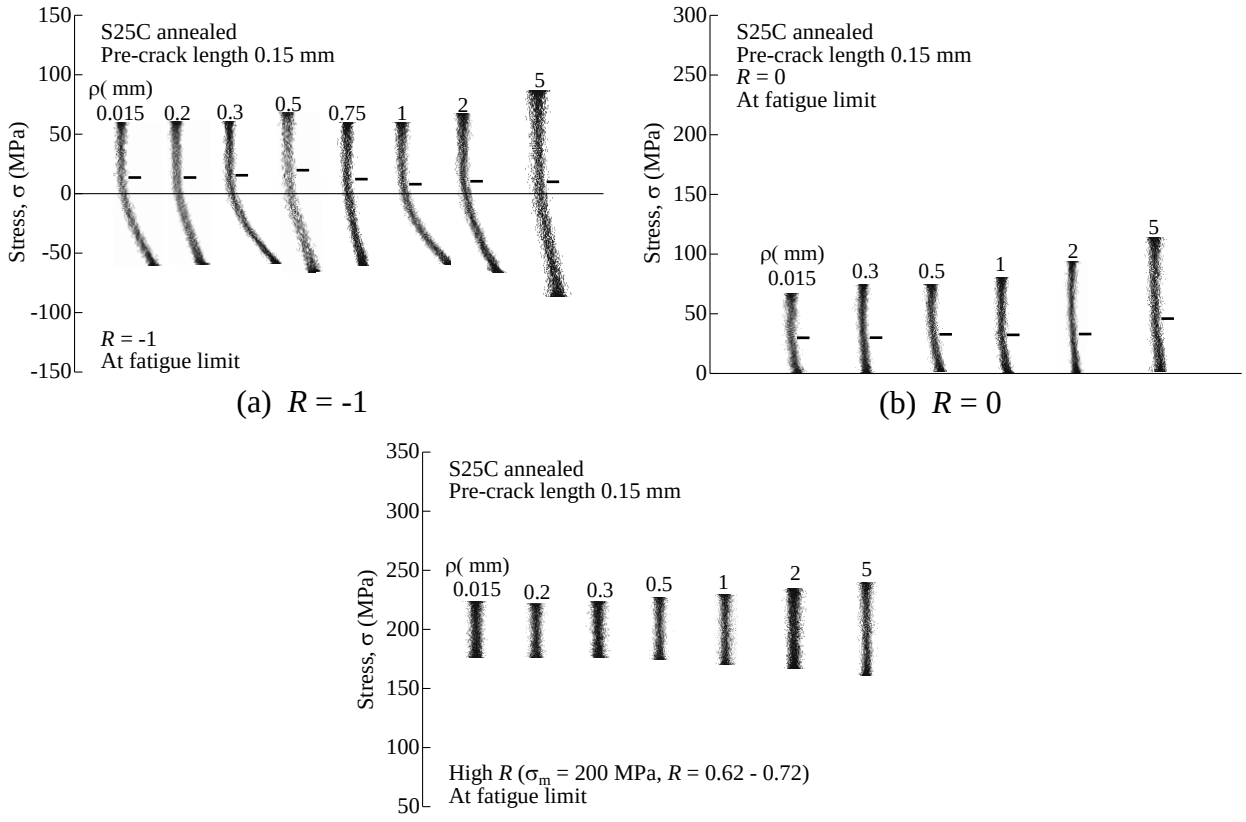

(a) R = -1 (b) R = 0

(c) High R

Fig. 5 Stress-offset displacement curves for the arrested crack at the fatigue limit.

Concept for achieving fatigue limit. After finishing the fatigue test at the fatigue limit, the fracture surface of the unbroken specimens was opened to measure the crack length. For R = -1 and R = 0, the crack length in the fatigue limit specimens was longer than the pre-crack length. Thus, the fatigue limit of the pre-cracked specimen for R = -1 and R = 0 was achieved by crack arrest. Figure 8 shows a model to achieve the fatigue limit of the pre-cracked specimen based on the crack arrest due to the development of crack closure with crack growth. Since the stress amplitude was constant in this test, the maximum stress intensity factor, K_{max}, increases with the crack propagation. The crack opening stress intensity factor, K_{op}, increases if crack closure occurs with crack growth. Consequently, $(\Delta K_{eff})_{th}$, which is defined by $K_{max} - K_{op}$, can be changed by the crack growth. On the other hand, there is a region where the crack cannot propagate because the stress intensity factor range is less than $(\Delta K_{eff})_{th}$. This non-propagating crack zone is shown by the shading in the figure. As shown in Fig. 8 by the bold curve, when K_{op} increase with the crack growth and reaches the shaded zone, the crack will be a non-propagating crack. In contrast, as shown in the figure by the bold dotted curve, if K_{op} remains below the shaded zone, the crack growth continues toward specimen failure. Therefore when the increase in K_{op} is relatively low, K_{max} should be low in order to achieve crack arrest. In other words, when the development of crack closure is minor, the fatigue limit is reduced and ΔK_{th} decreases.

Figure 9 show the results of the evaluation of the test by applying this model. As shown in Figs. (a) and (c), in which no failure of the specimen occurred, K_{op} increases with the crack extension, and then it went into the $(\Delta K_{eff})_{th}$ zone. This means that the crack becomes a non-propagating crack, and then the fatigue limit was achieved. On the other hand, as shown in Figs. (b) and (d) in which the specimens were broken, K_{op} remained below the $(\Delta K_{eff})_{th}$ band.

Effects of notch root radius ρ and stress ratio *R* on crack opening stress intensity factor K_{op}. The change in K_{op} with crack extension was examined based on the model shown in Fig. 8 to interpret the change in ΔK_{th} depending on ρ shown in Fig. 3. The results are shown in Fig. 10. In this part, two notch root radii (ρ = 0.015 and ρ = 0.5 mm) were adopted as relatively sharp notches, and two other notch root radii (ρ = 1 mm and ρ = 5 mm) were used as relatively dull ones.

For R = -1, K_{op} was negative at the beginning of the crack propagation. This means that a crack was open even when the stress was compressive. In the dull notches, the increase in K_{op} was suppressed compared to that of the sharp notches. In addition, K_{op} at crack arrest, which is called $(K_{op})_{th}$ that is denoted by the arrows in Fig. 10, was lower in the dull notches than in the sharp notches. This difference in $(K_{op})_{th}$ depending on ρ is directly related to the reduction in ΔK_{th} which is shown in Fig. 4. This result was consistent with the change in ΔK_{th} as ρ changed.

On the other hand, for R = 0, the change in K_{op} was almost the same for both the dull and sharp notches. This resulted in little difference in $(K_{op})_{th}$ between the dull and sharp notches.

The change in $(K_{op})_{th}$ with the change in ρ for R = -1 and R = 0 are shown in Fig. 11. The change in $(K_{op})_{th}$ was similar to the change in ΔK_{th} which is shown in Fig. 4. The $(K_{op})_{th}$ of the relatively dull notches was lower than that of the sharp notches, and this is the reason for the reduction in ΔK_{th} for R = -1.

Summary

The fatigue crack propagation behavior of a 0.15mm deep short pre-crack at the root of a long notch was investigated in terms of the effect of the notch root radius and the stress ratio on the crack propagation threshold, ΔK_{th}. The results are as follows:

(1) For R = -1, ΔK_{th} for a relatively dull notch was lower than that for a relatively sharp notch. This was caused by the difference in the increase in K_{op} depending on ρ.

(2) For the stress ratio greater than 0, ΔK_{th} was constant regardless of the notch root radius.

(3) The $(\Delta K_{eff})_{th}$ values were constant for all the test conditions. The change in ΔK_{th} depending the notch root radius, ρ, shown for R = -1 can be explained by the crack closure behavior.

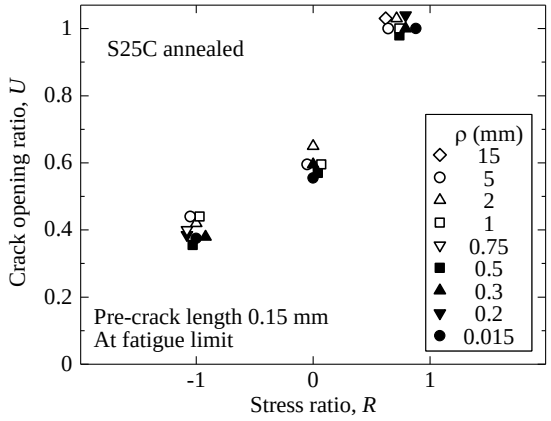

Fig. 6 Effect of stress ratio R on crack opening ratio U for arrested crack at fatigue limit.

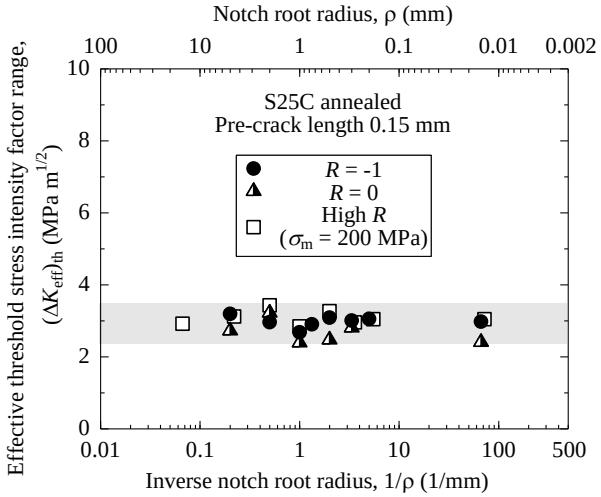

Fig. 7 Effects of notch root radius ρ and stress ratio R on effective threshold stress intensity factor range $(\Delta K_{eff})_{th}$.

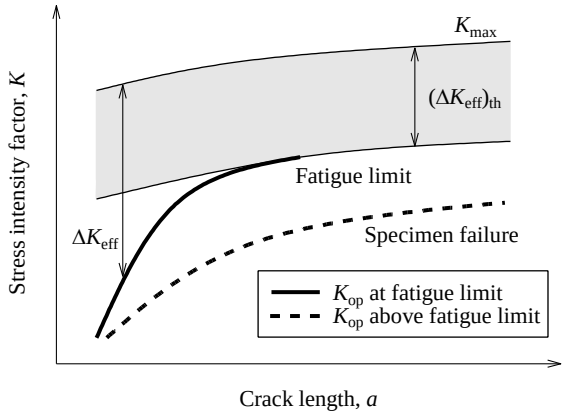

Fig. 8 Concept for achieving fatigue limit.

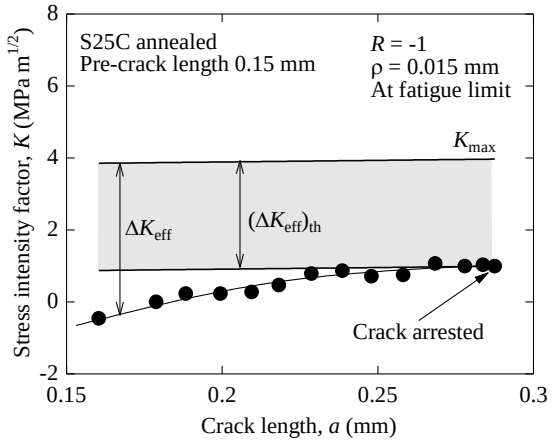

(a) At fatigue limit (ρ = 0.015 mm)

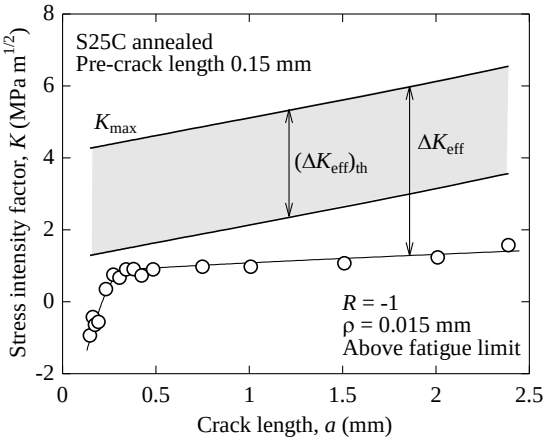

(b) Above fatigue limit (ρ = 0.015 mm)

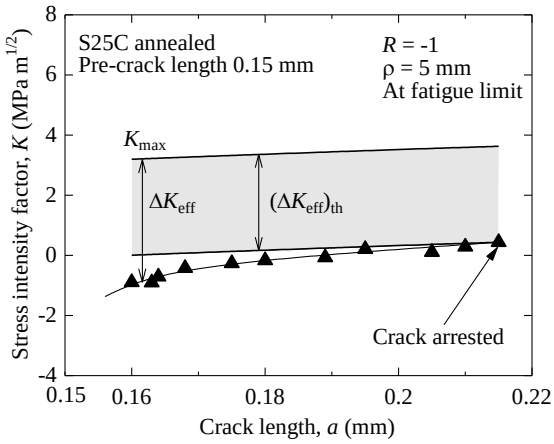

(c) At fatigue limit (ρ = 5 mm)

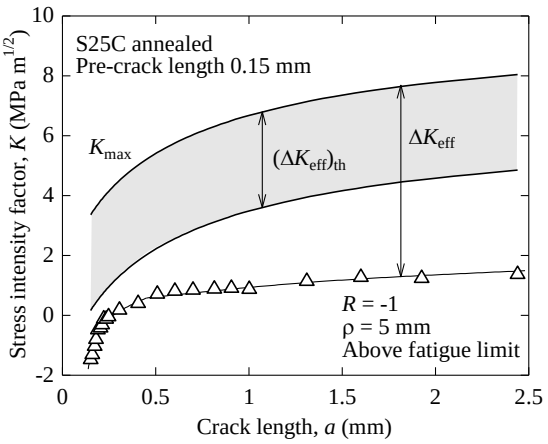

(d) Above fatigue limit (ρ = 5 mm)

Fig. 9 Evaluation of fatigue limit based on our model.

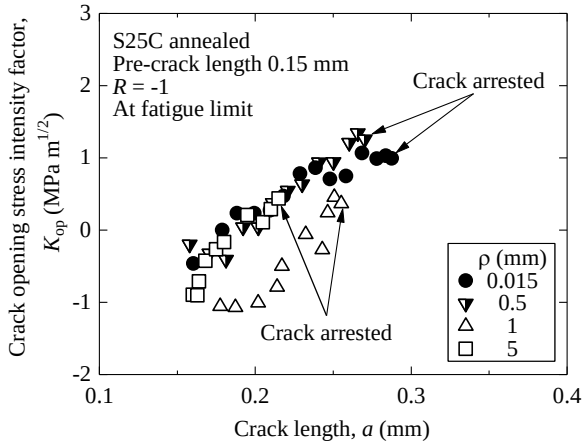

(a) R = -1

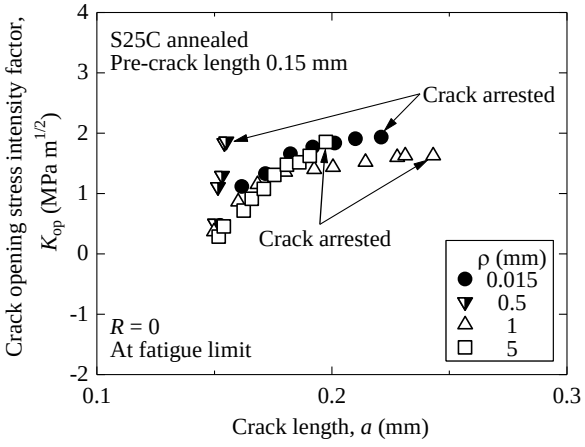

(b) R = 0

Fig. 10 Development of crack closure for R = -1 and R = 0 at the fatigue limit specimens.

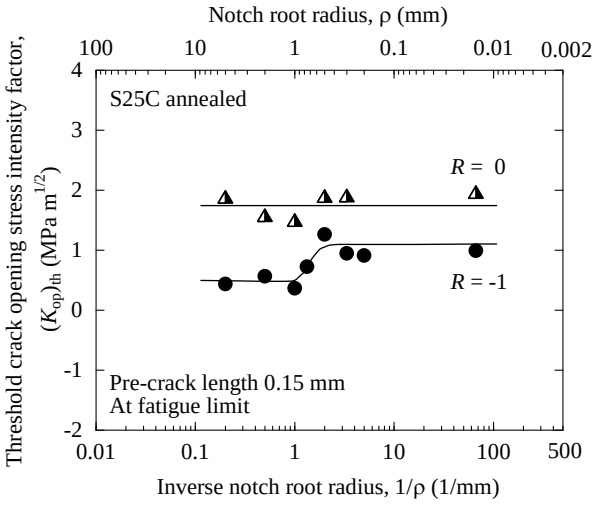

Fig. 11 Effects of notch root radius ρ and stress ratio R on threshold crack opening stress intensity factor $(K_{op})_{th}$.

Acknowledgement

This work has been supported by the NEDO project "Fundamental Research Project on Advanced Hydrogen Science" (2006-2012). This work was also supported by the World Premier International Research Center Initiative (WPI), MEXT, Japan. International Institute for Carbon-Neutral Energy Research (WPI-I2CNER) is supported by the World Premier International Research Initiative (WPI), MEXT, Japan.

References

[1] Pearson, S., *Engineering Fracture Mechanics*, Vol.7, (1975), pp.235-247.
[2] Kitagawa, H. and Takahashi, S., *Transaction of the Japan Society of Mechanical Engineers, Series A*, Vol.45, No.399, (1979), pp.1289-1303.
[3] Kondo, Y., Sakae, C., Kubota, M., Kudou, T., *The Society of Materials Science, Japan*, Vol.53, No.6, (2004), pp.661-666.
[4] Kondo, Y., Sakae, C., Kubota, M. and Kashiwagi, M., *Journal of ASTM International*, Vol.2, No.4, (2005), pp.415-432.
[5] Endo, M. and McEvily, A.J., *Materials Science and Engineering A*, 468–470, (2007), pp.51-58.
[6] Kikukawa, M., Jono, M., Tanaka, K. and Takatani, M., *Journal of Materials Science, Japan*, Vol. 25 (1976), pp.899-903.
[7] Gross, B. and Srawley, J.E., *NASA TN* D-2603, (1965).
[8] Lukas, P. and Klesnil, M., *Materials Science and Engineering*, 34-1, (1978), pp.61-66.
[9] Nakai, Y., Tanaka, K. and Kawashima, R., *The Society Science, Japan*, (1983), pp. 535-541.
[10] Elber, W., *Damage Tolerance in Aircraft Structures, ASTM STP* 486, (1971), pp.230-242.
[11] Nishitani, H., "Non-Propagating Crack", *The Society of Materials Science, Japan*, (1976), pp.296-306.
[12] El Haddad, M. H., Topper, T. H. and Smith, K. N., *Engineering Fracture Mechanics*, Vol. 11, (1979), pp.573-584.
[13] Takao, K., Nishitani, H., *The Society of Materials Science, Japan*, (1986), pp.1060-1064.
[14] Akiniwa, Y. and Tanaka, K., *Transaction of the Japan Society of Mechanical Engineers, Series A*, Vol. 53, No. 487, (1987), pp.393-400.